Nature Environment and Pollution Technology
An International Quarterly Scientific Journal

p-ISSN: 0972-6268
e-ISSN: 2395-3454

Vol. 18 | No. 4 | pp. 1375-1380 | 2019

Original Research Paper | Open Access

Adsorption Kinetics and Isotherms of Cr(VI) Ions in Aqueous Solution by Biochar Derived from *Torreya grandis* Nutshell

Chengcai Huang, Rui Qin, Linli Zhang, Muqing Qiu and Linfa Bao†
College of Life Science, Shaoxing University, Shaoxing, 312000, P.R. China
†Corresponding author: Linfa Bao

Nat. Env. & Poll. Tech.
Website: www.neptjournal.com

Received: 19-03-2019
Accepted: 01-06-2019

Key Words:
Cr(VI)
Biochar
Torreya grandis nutshell
Adsorption of heavy metals
Adsorption kinetics

ABSTRACT

Biochar is thought to be a good adsorption material for the adsorption of heavy metals. In this study, biochar derived from *Torreya grandis* nutshell was prepared through to be pyrolyzed under oxygen limited conditions in a muffle furnace. The adsorption experiments of Cr(VI) were carried out. Through Elemental Analyzer, Specific Surface Area Meter, Scanning Electron Microscopy, Transmission Electron Microscopy and Fourier Transform Infrared Spectroscopy, a fundamental understanding of the physical and chemical properties of biochar was gained. The results showed that it was a smooth sheet and irregular arrangement structure. The elements of C, H, O and N of biochar are 45.21%, 5.18%, 46.16% and 3.45% respectively. BET specific surface area of biochar is 42.24 m^2/g. A lot of oxygen-containing functional groups (– OH, COO –, – C – OH and so on) appeared on the surface of biochar. It can be described by the pseudo-second order kinetic rate model and Langmuir isotherm model. The adsorption process is a monolayer chemical process. The adsorption mechanism of biochar on heavy metal Cr(VI) contains the electrostatic attraction between biochar and $Cr_2O_7^{2-}$, $HCrO_4^-$ and CrO_4^{2-} ions in aqueous solution and complexation reaction of oxygen-containing functional groups (– OH, – COOH and so on) and $Cr_2O_7^{2-}$, $HCrO_4^-$ and CrO_4^{2-} ions on the surface of biochar.

INTRODUCTION

The metal of chromium and its compounds are a kind of toxic pollutants (Barrera-Díaz et al. 2012). The Cr(III) and Cr(VI) mainly exist in the environment. Cr(III) ions are relatively stable and less toxic (Litter 2015). However, Cr(VI) ions in aqueous solution have high solubility, the strong mobility, high toxicity and harmful to organisms. The concentration of Cr(VI) ions discharged from industries range from 0.1 to 100 mg/L. It is very important and urgent to treat Cr(VI) wastewater effectively (Xu et al. 2013, Du et al. 2015). At present, the treatment of Cr(VI) wastewater mainly includes chemical precipitation, redox, ion exchange, adsorption and so on. Among these treatment methods, the adsorption is widely applied into the treatment of wastewaters because of its high selectivity, economy, efficiency, simple operation and so on (Wang et al. 2016, Hu et al. 2017a).

Biochar is a good adsorption material for the adsorption of heavy metals. Biochar has a porous structure, and a lot of oxygen functional groups, such as hydroxyl, carboxyl, phenolic functional groups and so on, appear at the surface of biochar (Regmi et al. 2012, Wang et al. 2015, Park et al. 2018, Kretschmer et al. 2019). These oxygen functional groups are important for the adsorption of heavy metals. Some earlier researches showed that the adsorption mechanism of biochar on heavy metals involved electrostatic attraction, ion exchange, physical adsorption, complexation, precipitation, and a combination of multiple forces (Tong & Xu 2013, Ding et al. 2016, Park et al. 2016, Qiu et al. 2018, Hu et al. 2019). However, the adsorption mechanism for adsorption of different heavy metals is also different (Wang et al. 2015). Raw materials and pyrolysis temperature are important factors affecting the physical and chemical properties of biochar (Dutta et al. 2018, Mu et al. 2019). The adsorption capacity and characteristics of biochar for heavy metals are related to these properties. Biochar is usually prepared from terrestrial lignocellulosic materials and contains high content of carbon (Du et al. 2019). In China, the biomass resources are rich, such as peanut shells, straw, *Torreya grandis* nutshell, orange peel and so on. Most of them are burned directly, and not utilized effectively. It not only wastes resources, but also pollutes the environment. How to utilize them effectively is an urgent problem (Shen et al. 2015, Montesinos et al. 2016).

Torreya grandis is mainly grown in the relatively humid areas of southern China and distributed in Anhui and Zhejiang Provinces. Every year, a number of *Torreya grandis* nutshells are produced. In this work, *Torreya grandis* nutshell was chosen as the adsorbent. The foremost

objective of this research was to test the ability of biochar derived from *Torreya grandis* nutshell to remove Cr(VI) from aqueous solutions. Additionally, the other objectives are: (1) to gain a fundamental understanding of the physical and chemical properties of biochar derived from *Torreya grandis* nutshell; (2) to study the adsorption characteristics of Cr(VI) ions by biochar; and (3) to explore the adsorption mechanism of biochar on Cr(VI) ion in aqueous solutions.

MATERIALS AND METHODS

Preparation of Biochar

Torreya grandis nutshell was collected from croplands in a suburb of Shaoxing, China. The *Torreya grandis* nutshell samples were dried at room temperature and ground to pass through a 0.83 mm sieve. These *Torreya grandis* nutshell samples were used as feedstock for producing biochar. The ground *Torreya grandis* nutshell samples were placed in ceramic crucibles, covered with a tightly fitting lid and pyrolyzed under oxygen limited conditions in a muffle furnace. The pyrolysis temperature was 300°C and time was 4 h. Then, cooling at room temperature, biochars were ground to pass through a 0.25 mm sieve before adsorption experiments.

Characterization of Biochar

The elements of C, H, O and N were determined by Elemental Analyzer (Vario ELIII, Elementar, Germany). BET specific surface area was measured by specific surface area meter (Autosorb-iQ3). The particle microstructure of biochar was determined by Scanning Electron Microscopy (JEOL 6500F, Japan) and Transmission Electron Microscopy (JEM-F200, Japan). The functional groups on the surface of biochar were determined by Fourier Transform Infrared Spectroscopy (Bruker Tensor 27).

Adsorption Experiments

Adsorption experiments were carried out at room temperature. 0.2 g of biochar was added to the 250 mL of Erlenmeyer flask containing 50mL of 50mg/L Cr(VI) ions. pH of the solution was adjusted by 0.1 mol/L HCl or 0.1 mol/L NaOH. After the adsorption process reached the equilibrium, samples were taken out. The samples were centrifuged at 3000 r/min for 10 min, filtered through 0.45 μm filter and analyzed by atomic absorption method.

In the experiment of adsorption kinetics, the reaction time was 10, 20, 40, 60, 80, 120, 160, 200, 240, 280 and 360 min respectively. pH in solution was 2.0.

In the experiment of isothermal adsorption, the initial concentration of Cr(VI) ranged from 10 to 100 mg/L. pH in solution was 2.0, and the samples were determined at adsorption equilibrium.

Analytical Methods

The concentration of Cr(VI) was determined by atomic absorption method. The removal rate of Cr(VI) was calculated as following:

$$Q = \frac{C_0 - C_t}{C_0} \times 100\% \quad \ldots(1)$$

Where C_0 and C_t (mg/L) are the initial and equilibrium concentrations of Cr(VI) in solution respectively. Q is the removal rate of Cr(VI).

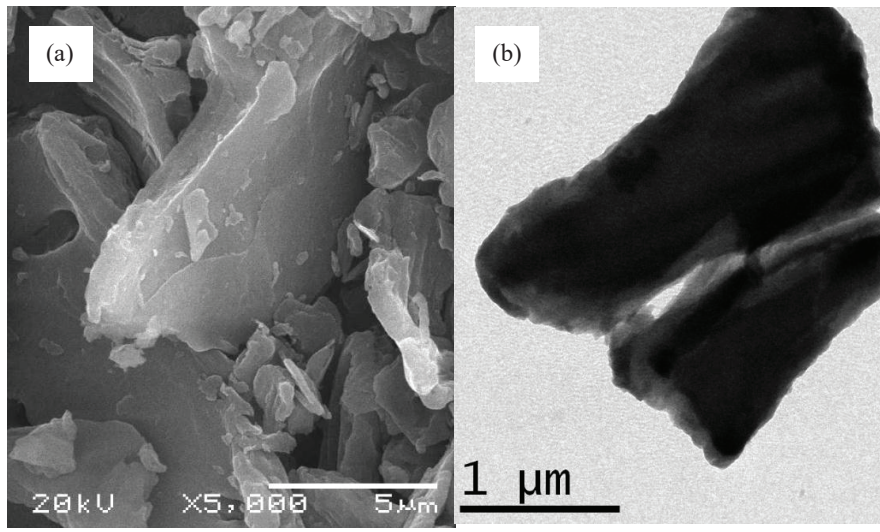

Fig. 1: SEM and TEM images of biochar, (a) SEM, (b) TEM.

Statistical Analyses of Data

All the experiments were repeated in duplicate and the result data were calculated as the mean with the standard deviation (SD). The value of the SD was calculated by Excel Software. All error estimates given in the text and error bars in figures are standard deviation of means (mean ± SD). All statistical significances were noted at α=0.05 unless otherwise stated.

RESULTS AND DISCUSSION

Characteristics of Biochar

The elements of C, H, O and N of biochar are 45.21%, 5.18%, 46.16% and 3.45%. BET specific surface area of biochar is 42.24 m^2/g. The large BET specific surface area means the high adsorption capacity. The SEM and TEM images of biochar are shown in Fig. 1.

As seen from the Fig. 1, the surface of biochar is a smooth sheet with irregular arrangement. It has a very few holes and mainly some debris particles.

The FT-IR spectra of biochar are shown in Fig. 2. From Fig. 2, it can be concluded that several bands were associated with oxygen functional groups appeared on the surface of biochar. The peaks of biochar at approximately 3903, 3422, 1512, 1401, 1060 and 612 cm^{-1} were assigned to the – *OH* stretching vibration of the – *OH* groups, the *COO*– groups, –*C*–*O* stretching vibration or bending vibration of –*C*–*OH* or *C*–*O* stretching and the finger print region which is related to phosphate and sulphur functional groups (Montesinos et al. 2016, Subramanian et al. 2018). In a word, there are a lot of oxygen functional groups on the surface of biochar.

Sorption Kinetics

The effect of reaction time on the removal rate of Cr(VI) by biochar is shown in Fig. 3.

As shown from Fig. 3, it can be concluded that the removal rate of Cr(VI) increases gradually as the reaction time increases. When the adsorption equilibrium is approached, the removal rate of Cr(VI) increases slowly. After the reaction time reached 120 min, the removal rate did not increase obviously. So, the adsorption equilibrium time is thought to be 120 min.

According to data from Fig. 3, the sorption kinetics was discussed in detail. In this experiment, the pseudo-first order and pseudo-second order kinetic rate models were evaluated to predict the removal rate of Cr(VI) ions by the biochar.

The pseudo-first order rate is given as (Hu et al. 2017b):

$$\ln(q_e - q_t) = \ln q_e - k_1 t \qquad \ldots(2)$$

The pseudo-second order rate is given as:

$$\frac{t}{q_t} = \frac{1}{k_2 q_e^2} + \frac{1}{q_e} t \qquad \ldots(3)$$

Where, q_e (mg/g) is the amount of adsorbed solute at

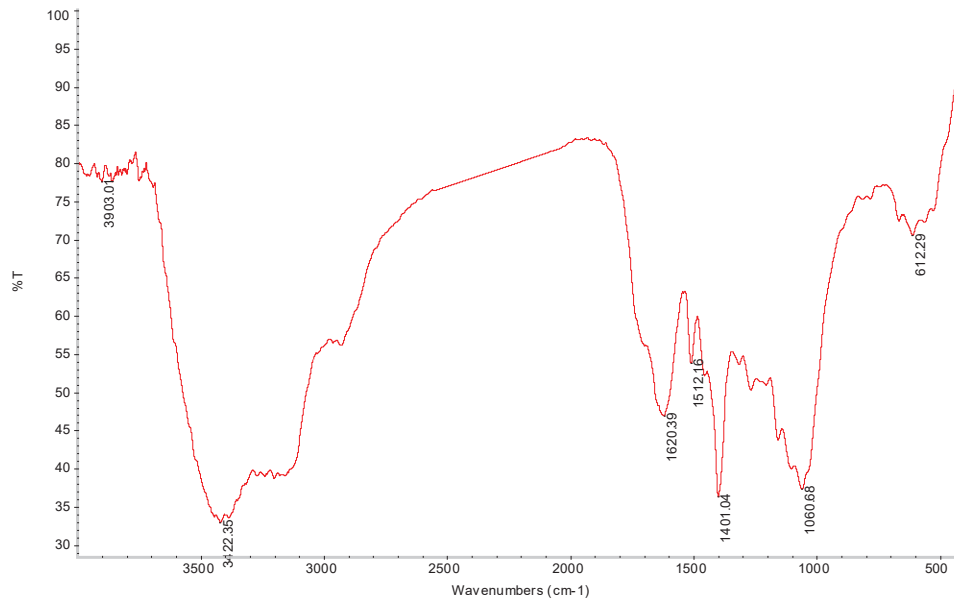

Fig. 2: FT-IR spectra of biochar.

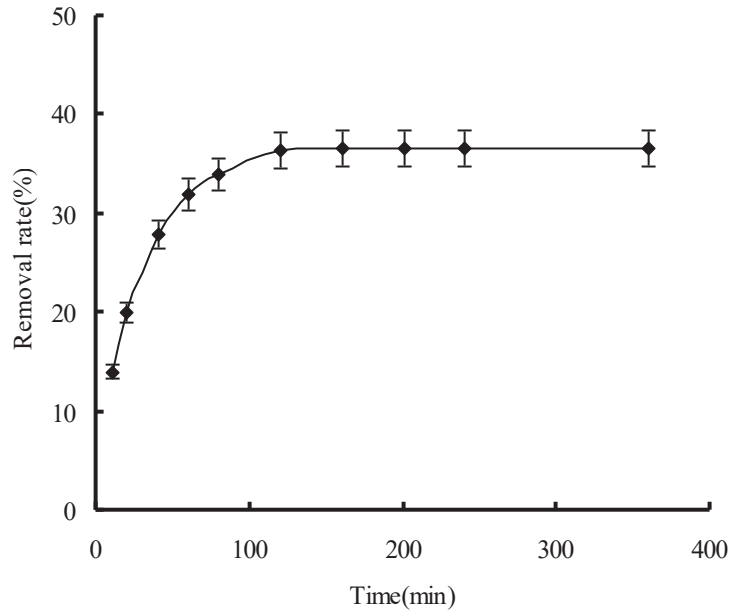

Fig. 3: The effect of reaction time on the removal rate of Cr(VI) by biochar.

equilibrium conditions, q_t (mg/g) is the amount of adsorbed solute at any time t (min), k_1 (h^{-1}) and k_2 (g/mg/h) are the model rate constant respectively.

Parameters of the pseudo-first order kinetic model and the pseudo-second order kinetic model for the description of Cr(VI) adsorption onto biochar are given in Table 1.

Table 1: Parameters of the pseudo-first order kinetic model and the pseudo-second order kinetic model for the description of Cr(VI) adsorption onto biochar.

pseudo-first order kinetic model			pseudo-second order kinetic model		
k_1 (min)	q_e (mg/g)	R^2	k_2 (mg/g·min)	q_e (mg/g)	R^2
0.49	4.62	0.892	0.21	4.95	0.998

From Table 1, it can be shown that the adsorption process fits well with the pseudo-second order kinetics model according to the value of R^2 (0.998 > 0.892). It also indicated that the adsorption of Cr(VI) by biochar is chemisorption process. The new compounds are formed on the surface of the adsorbent (Pozdnyakov et al. 2012).

Sorption Isotherm

The initial concentration of Cr(VI) was ranged from 10 to 100 mg/L. pH in solution is 2.0, and the samples were determined at 120 min. The experimental results are shown in Fig. 4.

In Fig. 4, the removal rate of Cr(VI) by biochar increases with the increase of initial concentration of Cr(VI), and adsorption reaches saturation eventually. It indicated that concentration gradient was the driving force for adsorption process. High concentration is benefitial for adsorption process. Further, the contact area and active sites on the surface of adsorbent are constant. At the first stage, Cr(VI) can be very rapidly adsorbed by biochar because of many adsorption sites. As the initial concentration of Cr(VI) increases, adsorption sites are utilized fully, and the adsorption process reaches saturation gradually.

According to data from Fig. 4, the sorption isotherms were determined. The Langmuir model and Freundlich model were used in this experiment. The Langmuir model and Freundlich model of linear forms are (Ameed & Ahmad 2009):

$$\frac{C_e}{q_e} = \frac{1}{K_L q_{max}} + \frac{C_e}{q_{max}} \quad \ldots(4)$$

$$\ln q_e = \ln K_F + \frac{1}{n} \ln C_e \quad \ldots(5)$$

Where, C_e (mg/L) is the equilibrium concentration in the solution, q_e (mg/g) is the adsorbate adsorbed at equilibrium, q_{max} (mg/g) is the maximum adsorption capacity, n is the Freundlich constant related to adsorption intensity, K_L (L/mg) and K_F ($(mg/g)^{1/n}$) are the adsorption constants for Langmuir and Freundlich models respectively.

Parameters of Langmuir isotherm model and Freundlich isotherm model for the description of Cr(VI) adsorption onto biochar are given in Table 2.

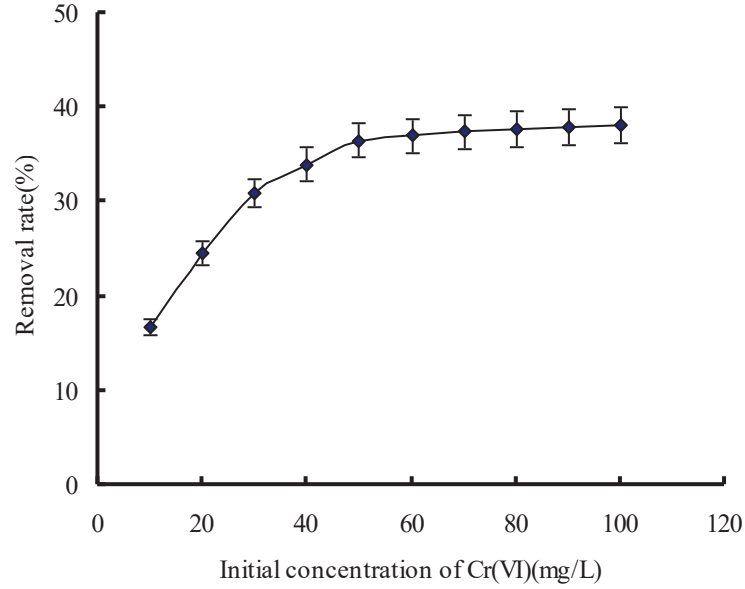

Fig. 4: The effect of the initial concentration of Cr(VI) on the removal rate of Cr(VI) by biochar.

Table 2: Parameters of Langmuir isotherm model and Freundlich isotherm model for the description of Cr(VI) adsorption onto biochar.

Langmuir			Freundlich		
q_m(mg/g)	K_L	R^2	K_F	n	R^2
5.12	0.03	0.999	1.24	0.18	0.812

From Table 2, Langmuir isotherm model can better describe the adsorption isothermal process of biochar on Cr(VI) according to the value of R^2 (0.999 > 0.812). The adsorption process is monolayer adsorption process.

Sorption Mechanism

Cr(VI) ions in aqueous solution mainly exists in the form of H_2CrO_4, $Cr_2O_7^{2-}$, $HCrO_4^-$ and CrO_4^{2-} in the environment. As the pH value in the solution is low, it mainly exists in the form of $HCrO_4^-$, a small amount of H_2CrO_4 and $Cr_2O_7^{2-}$. It is due to the presence of a large amount of H^+ ions in the solution, which leads to reaction of functional groups on the surface of the biochar with ions, such as H^+, $-OH$, $-COOH$ and so on. The positively charged of $-OH_2^+$ and $-COOH_2^+$ functional groups were appeared. These functional groups combine with $Cr_2O_7^{2-}$, $HCrO_4^-$ and CrO_4^{2-} through electrostatic interaction (Mohan et al. 2014). They were reacted with oxygen functional groups (–*OH*, –*COOH* and so on) appeared on the surface of biochar, and a lot of stable compounds were formed (Kołodyńska et al. 2012). So, it can be concluded that the adsorption mechanism of biochar on heavy metal Cr(VI) contains the electrostatic attraction and complexation reaction of oxygen functional groups.

CONCLUSIONS

1. The *Torreya grandis* nutshell can be effectively converted into the biochar, which can gain the goal of recycling waste resources. The obtained biochar derived from *Torreya grandis* nutshell is a smooth sheet and irregular arrangement structure. It has a large specific surface area and a lot of oxygen functional groups on the surface. So, it can be applied for the treatment of heavy metal.
2. The biochar can effectively remove Cr(V) in aqueous solution. It can be described by the pseudo-second order kinetic rate model and Langmuir isotherm model. The adsorption process is monolayer chemical process.
3. The adsorption mechanism of biochar on heavy metal Cr(VI) contains the electrostatic attraction and complexation reaction of oxygen functional groups.

ACKNOWLEDGEMENTS

This study was financially supported by the project of science and technology plan in Zhejiang Province (LGF19C030001) and the project of science and technology plan in Shaoxing City (2017B70058).

REFERENCES

Ameed, B.H. and Ahmad, A.A. 2009. Batch adsorption of methylene blue from aqueous solution by garlic peel, an agricultural waste biomass.

J. Hazard. Mater., 164: 870-875.

Barrera-Díaz, C.E., Lugo-Lugo, V. and Bilyeu, B. 2012. A review of chemical, electrochemical and biological methods for aqueous Cr(VI) reduction. J. Hazard. Mater., 223-224: 1-12.

Ding, Z.H., Hu, X., Wan, Y.S., Wang, S.S. and Gao, B. 2016. Removal of lead, copper, cadmium, zinc, and nickel from aqueous solutions by alkali-modified biochar: Batch and column tests. J. Indust. Eng. Chem., 33: 239-245.

Du, X.D., Yi, X.H., Wang, P., Zheng, W.W., Deng, J.G. and Wang, C.C. 2019. Robust photocatalytic reduction of Cr(VI) on UiO-66-NH_2(Zr/Hf) metalorganic framework membrane under sunlight irradiation. Chem. Eng. J., 356: 393-399.

Du, Y., Tao, Z., Guan, J., Sun, Z., Zeng, W., Wen, P., Ni, K., Ye, J., Yang, S., Du, P., and Zhu, Y. 2015. Microwave-assisted synthesis of hematite/activated graphene composites with superior performance for photocatalytic reduction of Cr(VI). RSC Adv., 5: 81438-81444.

Dutta, A.K., Ghorai, U.K., Chattopadhyay, K.K. and Banerjee, D. 2018. Removal of textile dyes by carbon nanotubes: A comparison between adsorption and UV assisted photocatalysis. Physica E Low Dimens. Syst. Nanost., 99: 6-15.

Hu, B.W., Qiu, M.Q., Hu, Q.Y., Sun, Y.B., Sheng, G.D., Hu, J. and Ma, J.Y. 2017a. Decontamination of Sr(II) on magnetic polyaniline/graphene oxide composites: Evidence from experimental, spectroscopic, and modeling investigation, ACS Sustain. Chem. & Eng., 5: 6924-6931.

Hu, B.W., Hu, Q.Y., Xu, D. and Chen, C.G. 2017b. The adsorption of U(VI) on carbonaceous nanofibers: A combined batch, EXAFS and modeling techniques. Sep. Pur. Technol., 175: 140-146.

Hu, B.W., Guo, X.J., Zheng, C., Song, G., Chen, D.Y., Zhu, Y.L., Song, X.F. and Sun, Y.B. 2019. Plasma-enhanced amidoxime/magnetic graphene oxide for efficient enrichment of U(VI) investigated by EXAFS and modeling techniques. Chem. Eng. J., 357: 66-74.

Kołodyńska, D., Wne˛ trzak, R., Leahy, J.J., Hayes, M.H.B., Kwapiński, W. and Hubicki, Z., 2012. Kinetic and adsorptive characterization of biochar in metal ions removal. Chem. Eng. J., 197: 295-305.

Kretschmer, I., Senn, A.M., Meichtry, J.M., Custo, G., Halac, E.B., Dillert R., Bahnemann D.W. and Litter, M.I. 2019. Photocatalytic reduction of Cr(VI) on hematite nanoparticles in the presence of oxalate and citrate. Appl. Catal. B: Environ., 242: 218-226.

Litter, M.I. 2015. Mechanisms of removal of heavy metals and arsenic from water by TiO_2-heterogeneous photocatalysis. Pure Appl. Chem., 87: 557-568.

Litter, M.I. 2017. Last advances on TiO_2-photocatalytic removal of chromium, uranium and arsenic. Curr. Opin. Green Sustain. Chem., 6: 150-158

Mohan, D., Kumar, H., Sarswat, A., Alexandre-Franco, M. and Pittman, C.U. 2014. Cadmium and lead remediation using magnetic oak wood and oak bark fast pyrolysis bio-chars. Chem. Eng. J., 236: 513-528.

Montesinos, V.N., Salou, C., Meichtry, J.M., Colbeau-Justin, C. and Litter, M.I. 2016. Role of Cr(III) deposition during the photocatalytic transformation of hexavalent chromium and citric acid over commercial TiO_2 samples. Photochem. Photobiol. Sci., 15: 228-234.

Mu, W.J., Du, S.Z, Li, X.L., Yu, Q.H., Wei, H.Y. and Yang, Y.C. and Peng, S.M. 2019. Removal of radioactive palladium based on novel 2D titanium carbides. Chem. Eng. J., 358: 283-290.

Park, M., Park, J., Kang, J.C., Han, Y. and Jeong, H.Y. 2018. Removal of hexavalent chromium using mackinawite (FeS)-coated sand. J. Hazard. Mater., 360: 17-23.

Park, S.H., Cho, H.J., Ryu, C. and Park, Y. 2016. Removal of copper(II) in aqueous solution using pyrolytic biochars derived from red macroalga Porphyra teners. J. Indust. Eng. Chem., 36: 314-319.

Pozdnyakov, I.P., Kolomeets, A.V., Plyusnin, V.F., Melnikov, A.A., Kompanets, V.O., Chekalin, S.V., Tkachenko, N. and Lemmetyinen, H. 2012. Photophysics of Fe(III)-tartrate and Fe(III)-citrate complexes in aqueous solutions. Chem. Phys. Lett., 530: 45-48.

Qiu, M.Q., Wang, M., Zhao, Q.Z., Hu, B.W. and Zhu, Y.L. 2018. XANES and EXAFS investigation of uranium incorporation on nZVI in the presence of phosphate. Chemosphere, 201: 764-771.

Regmi, P., Moscoso, J.L.G., Kumar, S., Cao, X.Y., Mao, J.D. and Schafran, G. 2012. Removal of copper and cadmium from aqueous solution using switchgrass biochar produced via hydrothermal carbonization process. J. Environ. Manage., 109: 61-69.

Shen, Z.T., Jin, F., Wang, F., McMilla,n O. and Al-Tabbaa, A. 2015. Sorption of lead by Salisbury biochar produced from British broadleaf hardwood. Biores. Technol., 193: 553-556.

Subramanian, G., Kumar, G.S.S., Ravi, V., Sundaresan, N.R. and Madras, G. 2018. Photochemical detoxification of Cr(VI) using iron and saccharic acid: Insights from cytotoxic and genotoxic assays. Environ. Sci. Water Res. Technol., 4: 1152-1162.

Tong, X.J. and Xu, R.K. 2013. Removal of Cu(II) from acidic electroplating effluent by biochars generated from crop straws. J. Environ. Sci., 25: 652-658.

Wang, D., He, S., Shan, C., Ye, Y., Ma, H., Zhang, X., Zhang, W. and Pan, B. 2016. Chromium speciation in tannery effluent after alkaline precipitation: Isolation and characterization. J. Hazard. Mater., 316: 169-177.

Wang, H.Y., Gao, B., Wang, S.S., Fang, J., Xue, Y.W. and Yang, K. 2015. Removal of Pb(II), Cu(II), and Cd(II) from aqueous solutions by biochar derived from $KMnO_4$ treated hickory wood. Biores. Technol., 197: 356-362.

Wang, S., Gao, B., Zimmerman, A.R., Li, Y., Ma, L., Harris, W.G. and Migliaccio, K.W. 2015. Removal of arsenic by magnetic biochar prepared from pinewood and natural hematite. Bioresour. Technol., 175: 391-395.

Xu, Z., Bai, S., Liang, J., Zhou, L. and Lan, Y. 2013. Photocatalytic reduction of Cr(VI) by citric and oxalic acids over biogenetic jarosite. Mater. Sci. Eng. C, 33: 2192-2196.